



Title	Photocatalytic activity of octahedral single-crystalline mesoparticles of anatase titanium(iv) oxide
Author(s)	Amano, Fumiaki; Yasumoto, Taikei; Prieto-Mahaney, Orlando-Omar; Uchida, Satoshi; Shibayama, Tamaki; Ohtani, Bunsho
Citation	Chemical Communications, 2009(17), 2311-2313 <a href="https://doi.org/10.1039/b822634b">https://doi.org/10.1039/b822634b</a>
Issue Date	2009
Doc URL	<a href="http://hdl.handle.net/2115/48662">http://hdl.handle.net/2115/48662</a>
Rights	Chem. Commun., 2009, 2311-2313 - Reproduced by permission of The Royal Society of Chemistry (RSC)
Type	article (author version)
File Information	ChemCommun2009_Ohtani.pdf



[Instructions for use](#)

# Photocatalytic Activity of Octahedral Single-Crystalline Mesoparticles of Anatase Titanium(IV) Oxide

Fumiaki Amano,<sup>\*a,b</sup> Taikei Yasumoto,<sup>b</sup> Orlando-Omar Prieto-Mahaney,<sup>b</sup> Satoshi Uchida,<sup>c</sup> Tamaki Shibayama,<sup>d</sup> and Bunsho Ohtani<sup>a,b</sup>

*Received (in XXX, XXX) Xth XXXXXXXXXX 200X, Accepted Xth XXXXXXXXXX 200X*

*First published on the web Xth XXXXXXXXXX 200X*

DOI: 10.1039/b000000x

Octahedral titanium(IV) oxide (TiO<sub>2</sub>) crystallites exposing anatase {101} facets exhibited relatively high photocatalytic activity for oxidative decomposition of organic compounds and low activity for hydrogen liberation in the absence of molecular oxygen probably due to the characteristics of anatase {101} surface.

Anatase has been the most studied polymorph of TiO<sub>2</sub> owing to its higher photocatalytic activity for oxidative decomposition of organic compounds in the presence of molecular oxygen,<sup>1,2</sup> hydrogen (H<sub>2</sub>) liberation, and so on. Surface free energy of anatase {101} lattice plane is reported to be the smallest among the other planes of anatase.<sup>3,4</sup> In agreement with natural minerals, a truncated octahedral bipyramid, exposing eight {101} facets as well as two {001} facets, has been shown as a thermodynamically most stable shape of anatase crystallites based on Wulff construction.<sup>3,4</sup> In spite of the important applications of anatase TiO<sub>2</sub>, experimental studies on the photoactive property of single-crystalline surface are still limited due to the difficulty to obtain high quality anatase samples.<sup>5</sup> A few studies suggested the significant role of facets of TiO<sub>2</sub> polyhedral particles for photocatalytic reactions.<sup>6,7</sup> Recent development of hydrothermal reaction method has enabled to prepare anatase crystalline particles with well-developed facets in a relatively high yield.<sup>8-10</sup> The aim of the present study is to investigate the roles of {101} facets, which is the most likely observed on anatase mesoparticles,<sup>11</sup> for practical photocatalytic reaction system such as powder suspensions. In order to compare the

photocatalytic activity of well-defined anatase single crystal particles with commercial TiO<sub>2</sub> photocatalyst powders, the crystalline size should be of submicrometer scale, mesoparticles, to have surface area comparable to commercial powders. We have found that hydrothermal reaction of titanate nanowires produced mesoparticles of anatase octahedral bipyramids. Their photocatalytic activity for oxidative decomposition of organic compounds and H<sub>2</sub> liberation from an aqueous methanol (MeOH) solution was investigated to clarify the photocatalytic property of anatase {101} facets.

Titanate nanowires were prepared by hydrothermal reaction of TiO<sub>2</sub> particles, P25 (Nippon Aerosil), in a 17-mol L<sup>-1</sup> potassium hydroxide solution at 383 K for 20 h.<sup>12</sup> The nanowires (100 mg) were stirred in a MilliQ-water (30 mL) and heated in a Teflon-lined autoclave (100 mL) at 443 K for 24 h. The white precipitates were centrifuged and dried at 393 K. Parts a–c of Fig. 1 show scanning electron microscopic (SEM) images of titanate nanowires before and after the hydrothermal reaction at 443 K. The typical diameter and length of titanate nanowires were 5–15 nm and several hundreds nanometers, respectively. Analysis using energy dispersive X-ray spectroscopy revealed the presence of potassium ion in titanate nanowires (atomic ratio of potassium to titanium; ca. 12%). Specific surface area (SSA) of titanate nanowires was ca. 400 m<sup>2</sup> g<sup>-1</sup>. Hydrothermal reaction of titanate nanowires resulted in a production of mesoparticles of an octahedral, i.e., bipyramidal shape, and their sizes of the long axis were < 100 nm. Proportion in number of the octahedral bipyramids among all particles was counted to be ca. 70%. The particles were of single crystal of anatase TiO<sub>2</sub> as found by high-resolution transmission electron microscopy (TEM) and selected area electron diffractometry (Fig. 1d and Fig. S1 in Supporting Information). The orientation of fringes, i.e., crystal direction, was consistent to that of the equilibrium shape of anatase crystallites. The octahedral bipyramids exhibited predominantly anatase {101} facets, while the edges of crystallites became rounded in some extent and other facets such as {100} were also exposed. Figure 2 shows X-ray diffraction patterns of titanate nanowires before and after hydrothermal reaction. The titanate phase was completely converted to anatase TiO<sub>2</sub> crystallites by hydrothermal reaction. There seemed to be no other TiO<sub>2</sub> polymorphs such as rutile. SSA

of the anatase particles containing octahedral crystallites was  $40 \text{ m}^2 \text{ g}^{-1}$ .

In the case when another source, tightly bound titanate nanowires, was employed as a precursor, larger octahedral particles ( $\text{SSA } 25 \text{ m}^2 \text{ g}^{-1}$ ) were obtained, and the size of the particles was not uniform. The average number of octahedral bipyramids was ca. 60% and lower than that of particles prepared from less-bundled titanate nanowires. This indicates that the nanowire structure gives influences on the process of octahedral crystallites production.

Photocatalytic activity of mesoparticles predominantly composed of octahedral crystallites for oxidative decomposition of organic compounds was evaluated by the rate of carbon dioxide ( $\text{CO}_2$ ) liberation from aerated aqueous suspension (5.0 mL) containing a photocatalyst (50 mg) under irradiation by a 400-W high-pressure mercury lamp ( $> 290 \text{ nm}$ ) at 298 K. Figure 3 shows relationship between photocatalytic activities in oxidative decomposition of acetic acid (AcOH, 5 vol%) and MeOH (50 vol%) in an aqueous solution containing the hydrothermally-prepared mesoparticles, P25 (composite of anatase (main) and rutile), and 19 commercial anatase  $\text{TiO}_2$  particles including JRC-TIO-1, 2, 7, 8, 9, 10, 12, and 13 (Catalysis Society of Japan), ST-01, 21, and 41 (Ishihara Sangyo), PC-101 and 102 (Titan Kogyo), TKP-101 and 102 (Tayca), and Hombikat UV100 (Sachtleben Chemie). The  $\text{CO}_2$ -liberation rate ( $r(\text{CO}_2)$ ) in decomposition of MeOH was lower than the  $r(\text{CO}_2)$  for decomposition of AcOH over all  $\text{TiO}_2$  photocatalysts. P25 and mesoparticles containing octahedral crystallites exhibited higher photocatalytic activity than those of commercial anatase  $\text{TiO}_2$  particles for both reactions. Roughly speaking,  $r(\text{CO}_2)$  in decomposition of MeOH was increased with an increase of  $r(\text{CO}_2)$  in decomposition of AcOH. We could not find any relationship between SSA and photocatalytic activity for oxidative decomposition of organic compounds among a series of anatase  $\text{TiO}_2$  samples. Although sole decisive factor for the higher  $r(\text{CO}_2)$  of octahedral mesoparticles has not been found, it is suggested that the presence of well-crystallized surface is significant for high level of photocatalytic activity for oxidative decomposition of organic compounds.

Figure 4 shows relationship between photocatalytic activities for oxidative

decomposition of MeOH and for dehydrogenation of MeOH. Photocatalytic dehydrogenation activity was evaluated by H<sub>2</sub> liberation rate ( $r(\text{H}_2)$ ) from a deaerated aqueous 50vol% MeOH solution containing hexachloroplatinic acid (2.0wt% as Pt) as a precursor of photodeposition of platinum. The  $r(\text{H}_2)$  of commercial anatase TiO<sub>2</sub> particles seems to increase along with an increase in  $r(\text{CO}_2)$  from a MeOH solution. For both reactions, P25 exhibited the highest photocatalytic activities. Although  $r(\text{CO}_2)$  of the mesoparticles containing octahedral crystallites was relatively high,  $r(\text{H}_2)$  from a MeOH solution was much slower than those of P25 and most commercial anatase TiO<sub>2</sub> particles. Since, for commercial anatase particles, we can see a tendency that the samples of high  $r(\text{CO}_2)$  from a MeOH solution shows high  $r(\text{H}_2)$  from a MeOH solution, the relatively low  $r(\text{H}_2)$  of octahedral-shaped mesoparticles seems strange. In contrast to photocatalytic dehydrogenation, photocatalytic oxidative decomposition was performed under aerated conditions. Therefore, it is suggested that photocatalytic activities were different between two reactions with and without molecular oxygen for octahedral crystallites. Considering the predominant exposure of characteristic facets on octahedral crystallites, the difference in photocatalytic activities was assumed to be related to the property of anatase {101} facets. It has been proposed that reduction of molecular oxygen by photoexcited electron and oxidation of organic compounds by positive hole are easily promoted on an anatase {101} facet.

In the case of photocatalytic dehydrogenation of MeOH,  $r(\text{H}_2)$  over anatase particles with small SSA was lower than that over nanoparticles with large SSA (Fig. S2). The SSA of the mesoparticles containing octahedral crystallites (25–40 m<sup>2</sup> g<sup>-1</sup>) was relatively smaller than those of commercial anatase particles. Therefore, one of the reason of the low  $r(\text{H}_2)$  over mesoparticles containing octahedral crystallites is their relatively small SSA. In general, crystals are grown in the direction to minimize overall surface free energy and higher energy facets disappear along with an increase of crystalline size,<sup>13,14</sup> so that anatase particles with relatively small SSA would expose predominantly low index facets with small energy, e.g., {101} and {100}. In this regard, the relatively low  $r(\text{H}_2)$  over anatase particles with small SSA might be related to the property of {101} facets,

which are likely exposed on well-grown crystallites. Another important point is that photocatalytic dehydrogenation of MeOH was performed in the presence of hexachloroplatinic acid, which is reduced by photoexcited electron to give platinum nanoparticles on TiO<sub>2</sub>. In the absence of platinum, H<sub>2</sub> liberation over anatase particles was negligible. Therefore, the  $r(\text{H}_2)$  would be influenced by not only the property of anatase crystallites but also the property of deposited platinum nanoparticles. In particular in low loading region, the photocatalytic activity for H<sub>2</sub> liberation may strongly depend on the state of deposited platinum particles. However, the dosage amount of platinum seemed sufficient (2.0 wt% as Pt) in the present study. We confirmed the deposition of platinum nanoparticles on octahedral bipyramids after photocatalytic dehydrogenation (Fig. S6). Furthermore, it was also confirmed that the platinum-loaded samples exhibited photocatalytic activity 3.4-times higher than that of the bare octahedral crystallites for oxidative decomposition of AcOH (Fig. S7). So that, the reason of low  $r(\text{H}_2)$  over mesoparticles containing octahedral crystallites is not attributable to difference in the state of the platinum nanoparticles but to difference in the properties of an anatase {101} facets with others such as reconstructed surface structures. Actually, theoretical and experimental studies have revealed that anatase {101} surface is less favorable for dissociative adsorption of water and MeOH to result in molecular non-dissociative adsorption.<sup>15-17</sup> The flatband potential of the {101} surface has been reported to locate positively by ca. 0.06 eV than that of the {001} surface, on which water molecules dissociatively chemisorbed.<sup>18</sup> Although energy level of conduction band bottom is one of the decisive factors for H<sub>2</sub> liberation, the difference of flatband potentials seems small among anatase lattice planes. Therefore, the low  $r(\text{H}_2)$  of octahedral crystallites might be due to the surface structure of anatase {101}, which would affect the reaction mechanism in molecular level, rather than the conduction band level.

In conclusion, both a preparation of anatase crystallites having a particular facet and an evaluation of the photocatalytic activity in practical powder-suspension system provided a new insight on photocatalytic property of anatase single-crystalline facets. It has been indicated that anatase {101} surface is effective for photocatalytic oxidative

decomposition of organic compounds in the presence of molecular oxygen. On the other hand, it was found that anatase {101} surface is not as effective as other surfaces exposed on ordinary anatase particles for H<sub>2</sub> liberation in the absence of molecular oxygen. Comparison of photocatalytic activity between mesoparticles exposing only one kind of facet and ones exposing particular two kinds of facets will give further information on the roles of specific lattice plane of anatase TiO<sub>2</sub> for photocatalytic reactions, which is in progress in our group.

One of us (FA) is grateful for Northern Advancement Center for Science and Technology, Japan for financial support.

### Notes and references

- 1) T. Ohno, K. Sarukawa and M. Matsumura, *J. Phys. Chem. B*, 2001, 105, 2417.
- 2) T. Torimoto, N. Nakamura, S. Ikeda and B. Ohtani, *Phys. Chem. Chem. Phys.*, 2002, 4, 5910.
- 3) M. Lazzeri, A. Vittadini and A. Selloni, *Phys. Review B*, 2001, 63, 155409.
- 4) U. Diebold, N. Ruzycki, G. S. Herman and A. Selloni, *Catal. Today*, 2003, 85, 93.
- 5) L. Kavan, M. Grätzel, S. E. Gilbert, C. Klemenz and H. J. Scheel, *J. Am. Chem. Soc.*, 1996, 118, 6716.
- 6) T. Ohno, K. Sarukawa and M. Matsumura, *New J. Chem.*, 2002, 26, 1167.
- 7) T. Taguchi, Y. Saito, K. Sarukawa, T. Ohno and M. Matsumura, *New J. Chem.*, 2003, 27, 1304.
- 8) H. G. Yang, C. H. Sun, S. Z. Qiao, J. Zou, G. Liu, S. C. Smith, H. M. Cheng and G. Q. Lu, *Nature*, 2008, 453, 638.
- 9) D. H. Wang, J. Liu, Q. S. Huo, Z. M. Nie, W. G. Lu, R. E. Williford and Y. B. Jiang, *J. Am. Chem. Soc.*, 2006, 128, 13670.
- 10) E. Hosono, S. Fujihara, H. Imai, I. Honma, I. Masaki and H. S. Zhou, *Acs Nano*, 2007, 1, 273.
- 11) V. Shklover, M. K. Nazeeruddin, S. M. Zakeeruddin, C. Barbe, A. Kay, T. Haibach, W. Steurer, R. Hermann, H. U. Nissen and M. Grätzel, *Chem. Mater.*, 1997, 9, 430.

- 12) *Jpn. Pat.*, P2005-162584A, 2005.
- 13) R. L. Penn and J. F. Banfield, *Geochim. Cosmochim. Acta*, 1999, 63, 1549.
- 14) Y. W. Jun, M. F. Casula, J. H. Sim, S. Y. Kim, J. Cheon and A. P. Alivisatos, *J. Am. Chem. Soc.*, 2003, 125, 15981.
- 15) G. S. Herman, Z. Dohnalek, N. Ruzycki and U. Diebold, *J. Phys. Chem. B*, 2003, 107, 2788.
- 16) Tilocca and A. Selloni, *J. Phys. Chem. B*, 2004, 108, 19314.
- 17) X. Q. Gong and A. Selloni, *J. Phys. Chem. B*, 2005, 109, 19560.
- 18) R. Hengerer, L. Kavan, P. Krtil and M. Grätzel, *J. Electrochem. Soc.*, 2000, 147, 1467.

<sup>a</sup> *Catalysis Research Center, Hokkaido University, Sapporo 001-0021, Japan. Fax: +81-11-706-9130; Tel: +81-11-706-9130; E-mail: amano@cat.hokudai.ac.jp*

<sup>b</sup> *Graduate School of Environmental Science, Hokkaido University, Sapporo 060-0810, Japan.*

<sup>c</sup> *Research Center for Advanced Science and Technology, The University of Tokyo, Tokyo 153-8904, Japan.*

<sup>d</sup> *Center for Advanced Research of Energy Conversion Materials, Hokkaido University, Sapporo 060-8628, Japan.*

† Electronic Supplementary Information (ESI) available: Experimental details, TEM image, effect of SSA on photocatalytic activity for dehydrogenation of MeOH, time courses of photocatalytic reactions, electron microscopic images of photodeposited platinum nanoparticles, and platinum loading effect on photocatalytic activity for AcOH decomposition. See DOI: 10.1039/b000000x/

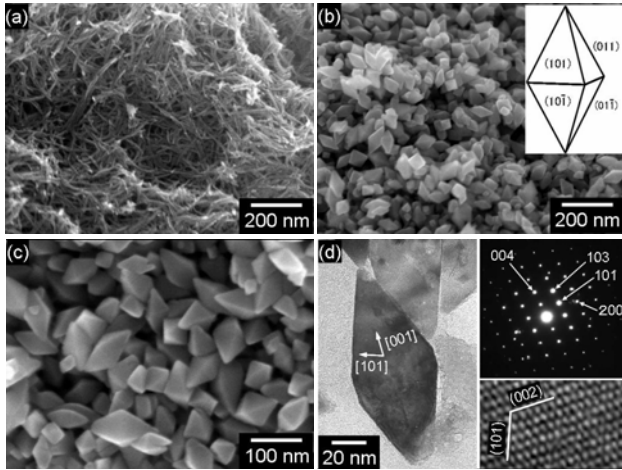


**Fig. 1** (a) SEM image of titanate nanowires. (b, c) SEM images of particles after hydrothermal reaction of titanate nanowires. (d) TEM image and electron diffraction pattern of an octahedral bipyramid.

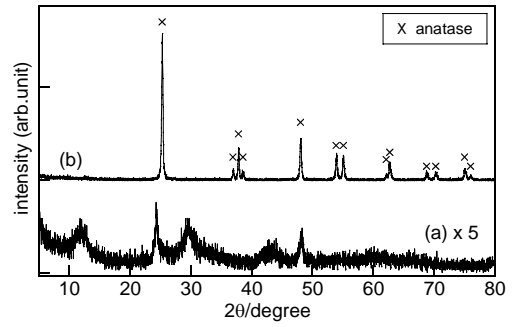


**Fig. 2** XRD patterns of (a) titanate nanowires and (b) particles after hydrothermal reaction of titanate nanowires. Pattern (b) was translated along a Y axis for clarity.

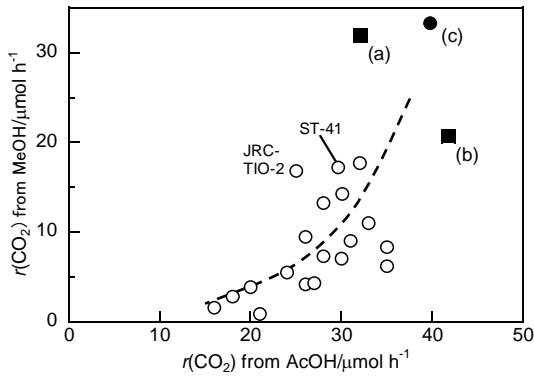


**Fig. 3** Relationship between photocatalytic activities for oxidative decomposition of AcOH and MeOH in an aqueous solution: (a, b) mesoparticles containing octahedral crystallites prepared from (a) titanate nanowires and (b) bundled titanate nanowires, (c) P25, and (open circle) commercial anatase  $\text{TiO}_2$  particles.

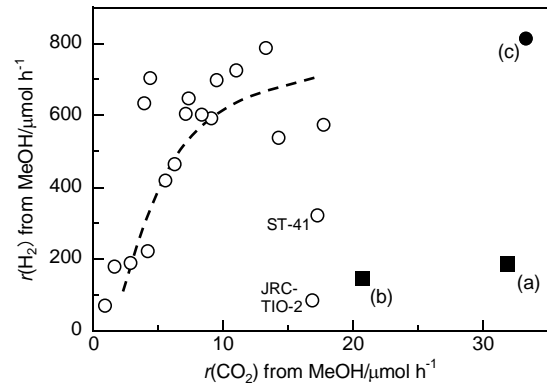


**Fig. 4** Relationship between photocatalytic activities for oxidative decomposition and dehydrogenation of MeOH in an aqueous solution. Symbols are the same as in Fig. 3.

